Molecular Crystals and Liquid Crystals
Publication details, including instructions for authors and subscription information:
http://www.tandfonline.com/loi/gmcl16

Studies on the Mesophases of OOBPD by X-Ray Diffraction Method

P. Mandal [a] , R. Paul [a] & S. Paul [a]
[a] Department of Physics, North Bengal University, Darjeeling

Version of record first published: 19 Oct 2010.

To cite this article: P. Mandal , R. Paul & S. Paul (1985): Studies on the Mesophases of OOBPD by X-Ray Diffraction Method, Molecular Crystals and Liquid Crystals, 131:3-4, 299-314

To link to this article: http://dx.doi.org/10.1080/00268948508085051

Mol. Cryst. Liq. Cryst., 1985, Vol. 131, pp. 299–314
0026-8941/85/1314–0299/$20.00/0

Printed in the United States of America

Studies on the Mesophases of OOBPD by X-Ray Diffraction Method

P. MANDAL, R. PAUL and S. PAUL

Department of Physics, North Bengal University, Darjeeling

(*Received March 26, 1984; in final form April 11, 1985*)

X-ray diffraction studies on the mesophases of OOBPD have been reported in this paper. This compound has four smectic phases and a nematic phase along with three crystalline phases. The smectic phases have been identified from texture study and from X-ray diffraction photographs of unoriented and magnetically oriented samples. Orientational distribution function $f(\beta)$ and order parameters $\langle P_2 \rangle$, $\langle P_4 \rangle$ for the nematic phase have been determined. Layer thickness, intermolecular spacings and tilt angles have also been calculated.

1. INTRODUCTION

Richly polymorphic homologous series Bis-(4, 4′-n-alkoxy-benzylidene)-1,4-phenylenediamines was investigated by many workers.[1–3] Phase transitions of the eighth member of the series, OOBPD, have also been studied by different workers[1–5] but no X-ray data of OOBPD have been reported so far. In this paper we have reported X-ray diffraction studies on OOBPD, the structural formula of which is

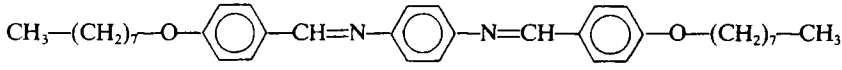

The transition temperatures obtained from Eastman Data service catalog (No. JJ14) are as follows:

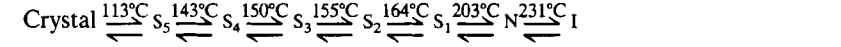

We, however, observed three different crystalline phases and four smectic phases along with the nematic phase, identification of the

phases were being done by X-ray diffraction photographs of powder and magnetically aligned samples and by texture studies. In the nematic phase orientational distribution function $f(\beta)$ and orientational order parameters $\langle P_2 \rangle$ and $\langle P_4 \rangle$ were calculated from the intensity distribution of the X-ray patterns. Intermolecular distances (D), apparent molecular length (l) or layer thickness (d) at different temperatures have also been calculated from diffraction data.

2. EXPERIMENTAL METHODS

The sample OOBPD was obtained from M/s Eastman Kodak & Co., Rochester, U.S.A. It was recrystallised from a concentrated solution of benzene and then dried over calcium chloride in vacuum desiccator. Transition temperatures were observed by us under polarizing microscope and also by DTA. The experimental set up used for X-ray studying of liquid crystals in a magnetic field has been described elsewhere.[6] We heated the sample to isotropic liquid and cooled it down very slowly to the desired temperature in presence of the magnetic field of .58 Tesla. Then photographs of the aligned samples were taken with X-rays perpendicular to the field direction, the magnetic field being used throughout the exposure time. Samples were malleable flakes, very difficult to pack. We failed to get monodomain samples in the smectic phases even after repeated attempts. Photographs of unoriented sample were taken by using a Universal Camera. The samples were contained in a thin walled glass capillary of approximately 1 mm diameter. The temperatures were measured and regulated with accuracy of ± 0.5°C with the help of a thermocouple inserted in the block containing the sample. Diffraction patterns in both the experimental set up were recorded on a flat plate film using Ni-filtered CuK_α radiation, with an exposure of about 5 to 6 hours. The photographs have two major diffraction maxima, the inner one having Bragg spacing of about 30 Å and the outer one of about 5 Å. The inner ring is related to the length of the molecule or smectic layer spacing and the outer ring arises due to interaction of the neighbouring molecules in a plane perpendicular to the molecular axis. In order to determine the various parameters the X-ray diffraction photographs were scanned, both linearly and circularly, by an optical densitometer (VEB Carl Zeiss Jena Model Microdensitometer 100) with auto recording facility. Measured optical densities were converted to X-ray intensities with the help of a calibration curve following Klug and Alexander.[7] The optical densities measured by cir-

cular scanning (along the arc of the outer ring) of the diffraction patterns were first converted to X-ray intensities as before and these intensity values $I(\theta)$ were then plotted at different azimuthal angular positions (θ). The background intensity arising due to the thermal vibration of the molecules and air scattering was eliminated from $I(\theta)$ versus θ curve before calculating order parameters $\langle P_2 \rangle$, $\langle P_4 \rangle$ and orientational distribution function $f(\beta)$ values from the intensity data. The quantities $\langle P_2 \rangle$, $\langle P_4 \rangle$ and β, $f(\beta)$ have been defined in section 3.3.

2.1 Texture studies

The melting behaviour was examined using polarizing microscope having a hot stage. Observations were performed under crossed polarizer with a magnification 150×. Solid crystals were melted on a clean glass surface and cover slip was used. Phase changes were observed at temperatures as given in the literature. These are also in good agreement with earlier observations. The textures observed can not be presented because we have no photographic arrangement. The compound on cooling from isotropic liquid showed a marbled texture, often found in nematic phase. Immediately below the nematic phase a tilted smectic phase was observed which exhibited a variant of marbled texture. This was found to be mobile by mechanical displacement of the cover slip. We identified S_1 to be a smectic C phase. S_2 phase is another tilted smectic phase which exhibited a variant of mosaic texture, so S_2 may be a S_F phase. On further cooling we got another tilted phase S_3 which showed a mosaic texture. Since the phase is tilted, this may be a S_G phase. S_4 phase showed a paramorphic mosaic texture, the same basic texture as in S_3 but with increased discontinuities and spontaneous flow at the boundaries of the blocks. This is like a S_H phase. Texture of S_5 was very difficult to identify. After repeated attempts we could get a fan shaped texture with spherulitic regions, paramorphosis from S_E fan shaped texture with concentric arcs. Since no flow was found this phase may be a solid like S_E or a solid. It is to be noted here that all the textures were observed during cooling, textures could not be observed distinctly during heating.

2.2 X-ray diffraction studies:

The diffraction photographs of the sample were taken at different temperatures starting from solid phase at room temperature to isotropic phase. The photographs were analysed to identify different

phases. In classifying the phases we followed the criteria proposed by de Vries[8] based on X-ray studies and not that by Sackmann[9] which was mainly based on miscibility study. We also followed the recommendation of Demus et al.[10] on the nomenclature of S_G and S_H.

Nematic phase was observed within the temperature range 203°C to 231°C. Aligned photograph at 207°C is shown in Figure 1. Since the intensity of the inner ring is far greater than that of the outer ring and since the next phase is a tilted smectic phase (S_C, see below) we infer that this may be a skewed cybotactic nematic phase which has been discussed in detail by de Vries.[14a,14b] We could not, however, confirm this because four discrete spots in the place of inner ring were not found in any of the several photographs taken (since we failed to get monodomain samples).

X-ray diffraction photographs within the range of 203°C to 143°C showed four smectic phases. Figure 2 shows that of S_1 phase having one sharp inner ring with two symmetrical spots at same Bragg spacing and a diffuse outer ring. The angle between the inner ring maxima and outer ring maxima of the aligned photograph at 185°C is found to be about 77° which shows that the molecules are inclined to the smectic planes. S_1 phase is thus a S_C phase, in conformity with the texture study.

Figure 3 is the aligned diffraction photograph of S_2 phase. The inner ring is spotted and the outer ring is sharp with six maxima, so S_2 phase may be S_F or S_I. First Diele[11] and then Gane[12b] established that structurally S_F and S_I phases differ only in the direction of tilt

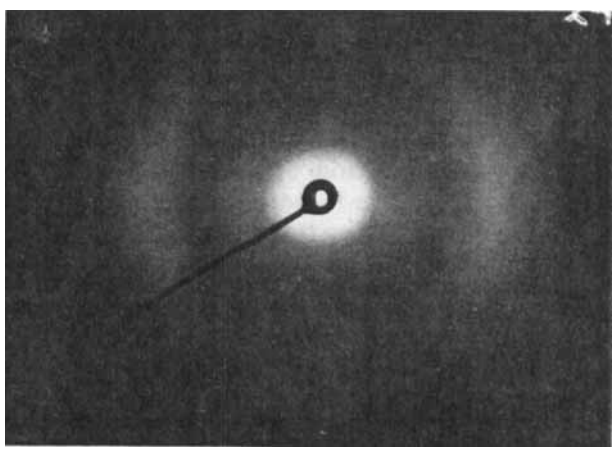

FIGURE 1 Aligned photograph of cybotactic Nematic phase at 207°C.

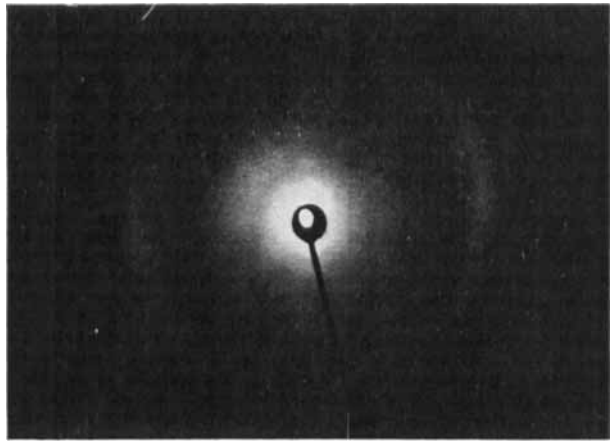

FIGURE 2 Aligned photograph of S_C phase at 185°C.

of the molecules relative to the pseudo-hexagonal packing in the plane normal to the molecular long axes—in S_F the tilt is directed towards an edge of the hexagon while in S_I it is directed towards an apex. A close look at the diffraction pattern suggests that it arises from a tilted pseudo hexagonal packing of the molecules and by indexing the photograph the unit cell is found to be a C-centered monoclinic with parameters $a = 6.67$ Å, $b = 9.88$ Å, $c = 37.48$ Å and $\beta = 121°$. So S_2 is a S_I phase ($b > a$).

Figures 4 and 5 are respectively powder and aligned photographs of S_3 phase. Figures 6 and 7 are those of S_4 phase. The powder

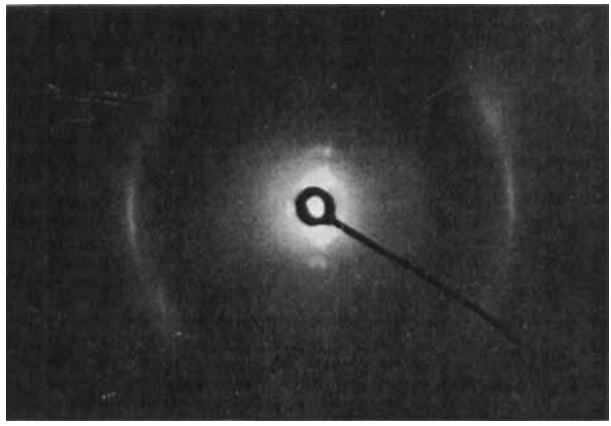

FIGURE 3 Aligned photograph of S_I phase at 160°C.

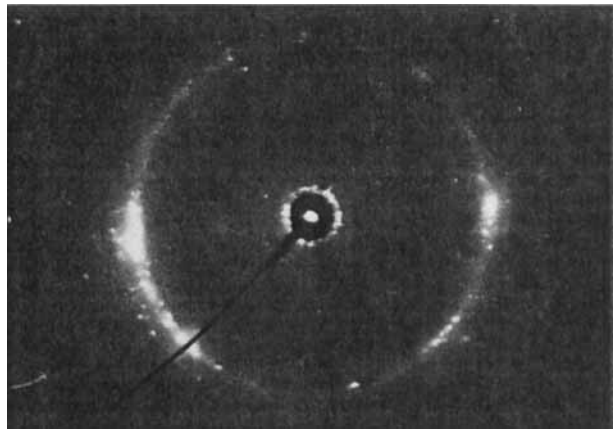

FIGURE 4 Powder photograph of $S_{G'}$ phase at 152°C.

photograph of S_3 shows several hkl reflections very closely spaced and in the aligned photograph (Figure 5), the diffraction maxima of S_I phase become spotted. These show clearly that S_3 is a long range three dimensional ordered tilted phase with pseudo-hexagonal packing within the layers. So S_3 is S_G phase or $S_{G'}$ phase as proposed by de Vries[12a] and Gane.[12b] In S_4 phase additional diffraction spots appear at higher angles showing the disappearance of C-centering as a result of quenching of the 6-fold rotational disorder of the molecules.[12b] So S_4 is S_H phase or $S_{H'}$ phase. Since the previous phase has S_I like tilt we presume that S_3 should be $S_{G'}$ and so S_4 should be $S_{H'}$,

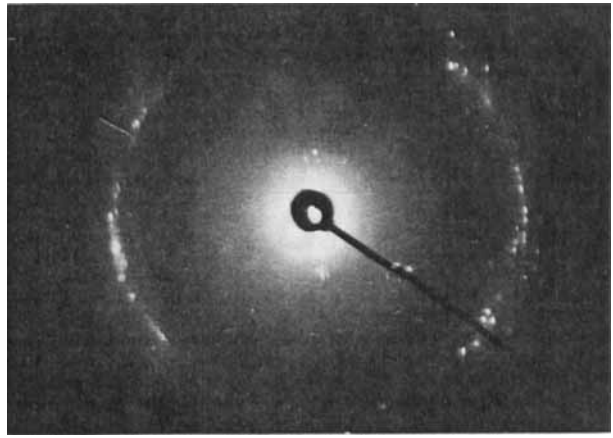

FIGURE 5 Aligned photograph of $S_{G'}$ phase at 152°C.

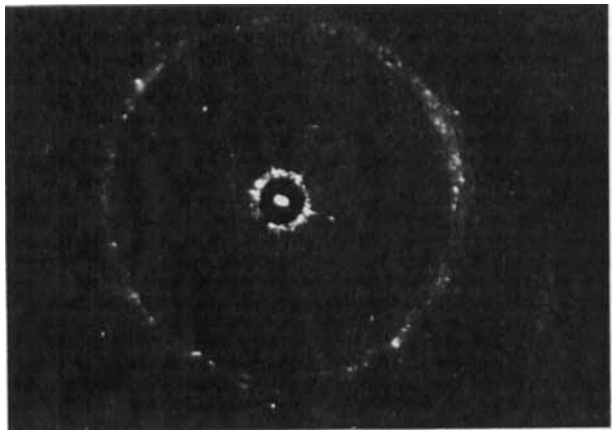

FIGURE 6 Powder photograph of $S_{H'}$ phase at 146°C.

of course, indexing the photographs and miscibility study would confirm this which could not be done by us. But we are sure that S_3 cannot be a S_B phase as proposed by Arora[5] because S_B is an orthogonal phase. It was earlier shown by Gane[12b] that S_3 cannot be a S_J phase as proposed by Gray[1]. In the seventh member of the series HEPTOBPD, Gane[12b] also identified these two phases as $S_{G'}$ and $S_{H'}$ but in a recent communication[13] they established them as Crystal J and K phases. Our DTA & Texture study however confirm them as smectics.

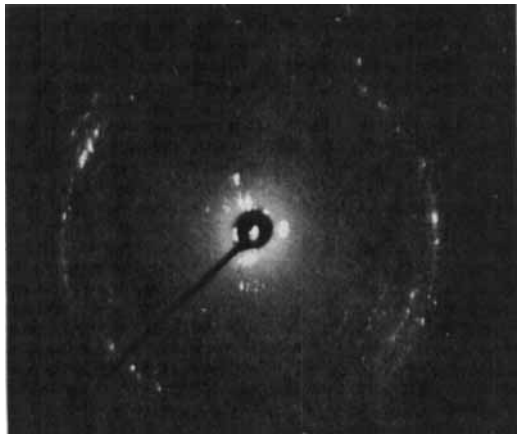

FIGURE 7 Aligned photograph of $S_{H'}$ phase at 146°C.

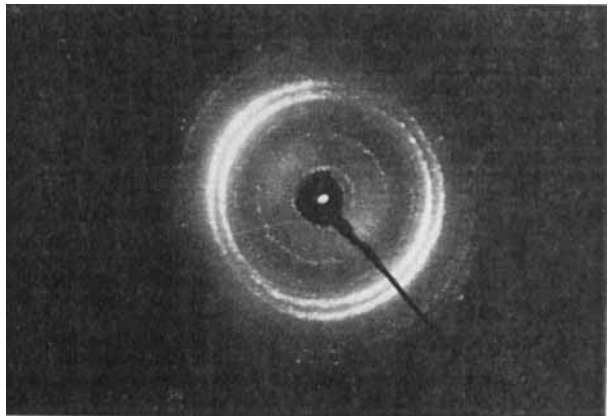

FIGURE 8 Powder photograph of Solid III phase at 133°C.

The diffraction patterns of the so-called 'S_5' modification are shown in Figure 8 (powder) and in Figure 9 (aligned). Arora[5] from miscibility study and Spratte[3] from DTA concluded that S_5 is a smectic phase. But the diffraction patterns clearly show that this phase is a solid phase which is in agreement with our texture study. Demus and Rurainski[4] also supported this observation from anomalous density study. Another solid phase transition was observed by us at 109°C (Figure 10). This transition had also been detected by Spratte.[3] The three solid phases were confirmed by noting the first Bragg spacings at different temperatures (d_1 = 4.18 Å at room temperature, 4.37 Å

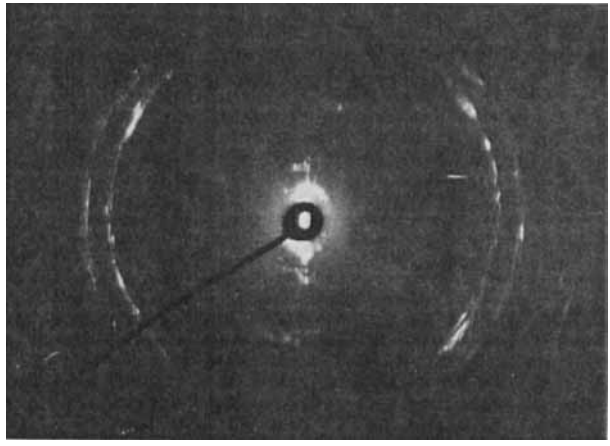

FIGURE 9 Aligned photograph of Solid III phase at 123°C.

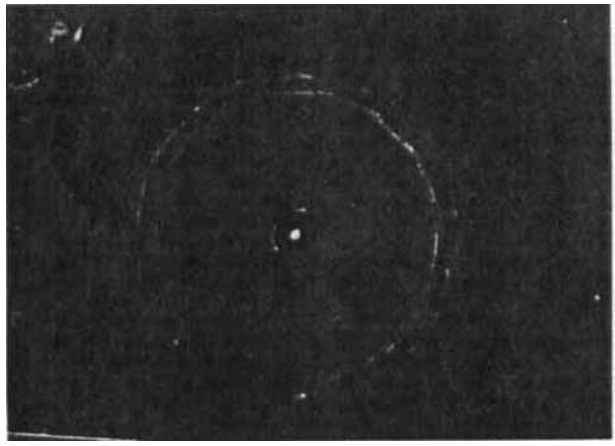

FIGURE 10 Powder photograph of Solid II phase at 111°C.

at 102°C, 4.26 Å at 111°C and 4.56 Å at 123°C). Figure 11 shows the room temperature photograph. Figure 12 is also a photograph at room temperature but with sample cooled from isotropic state in a magnetic field. In presence of magnetic field the sample aligned itself partially in the liquid crystalline phases and these alignment persists considerably even when cooled down to room temperature. Hence some characteristics of single crystal have appeared in Figure 12 in contrast to Figure 11. Here we must note that all the photographs are not in the same scale.

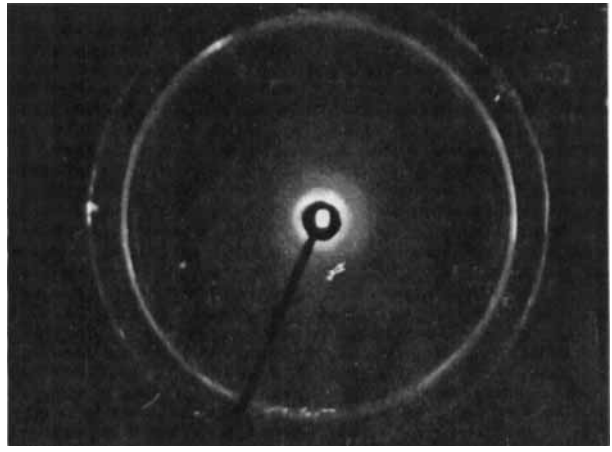

FIGURE 11 Powder photograph of Solid I phase at room temperature.

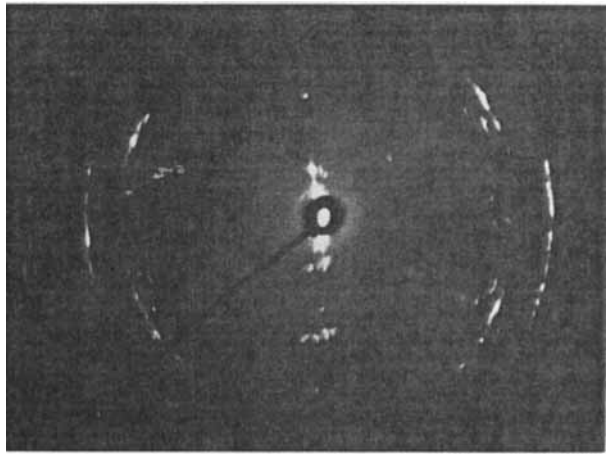

FIGURE 12 Magnetically treated room temperature photograph of Solid I phase.

3. RESULTS AND DISCUSSIONS

3.1 Different phases and their transition temperatures

From X-ray diffraction texture and DTA study the phase transitions of OOBPD are found to be as follows:

$$\text{Crystal I} \underset{}{\overset{109^{\circ}C}{\rightleftharpoons}} \text{Crystal II} \overset{113^{\circ}C}{\rightleftharpoons} \text{Crystal III} \overset{143^{\circ}C}{\rightleftharpoons} S_H' \overset{150^{\circ}C}{\rightleftharpoons} S_G'$$

$$I \underset{231^{\circ}C}{\rightleftharpoons} N_C \underset{203^{\circ}C}{\rightleftharpoons} S_C \underset{184^{\circ}C}{\rightleftharpoons} S_I \underset{155^{\circ}C}{\rightleftharpoons} S_G.$$

3.2 Intermolecular distances, layer spacings and tilt angles

Layer thickness (d) in case of smectic phases and apparent molecular length (l) in nematic phase have been calculated from the diffraction photographs using Bragg's formula. Intermolecular distances D have been determined only in nematic, S_I and S_C phases. In other two smectic phases D must be obtained from lattice constants which we could not calculate. In calculating D we used the formula[14b]

$$D = \frac{1.117\lambda}{2 \sin \theta}$$

Variation of D values with temperature for aligned sample is shown in Figure 13. Starting from a value of about 4.9 Å in the S_I phase it

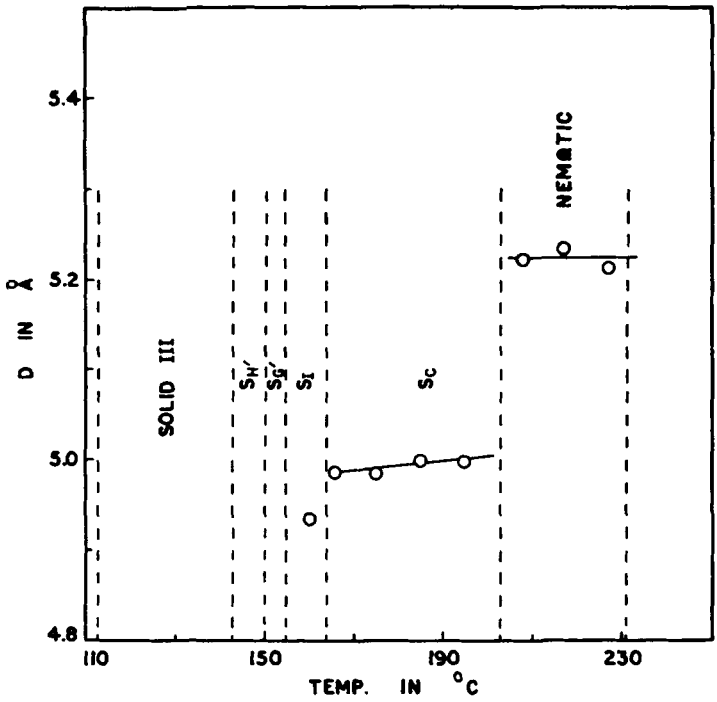

FIGURE 13 Variation of D with temperature for aligned sample.

rises to 5.2 Å in the nematic phase. In case on non-aligned sample the value of D has been found to be almost temperature independent, the average intermolecular distance being about 5.1 Å.

Variation of d and l with temperature, for aligned samples is shown in Figure 14. The temperature dependence of these parameters has been discussed by de Vries.[15,16] In our case d or l value is found to decrease with temperature. In the $S_{H'}$ phase d value is 33 Å and in the nematic phase l value is found to be 28 Å for aligned samples. But for non-aligned sample the variation is small, d being 30 Å in $S_{H'}$ phase and l being 29.3 Å in nematic phase. With the help of stereo model unit (Prentice Hall Inc., West Nyack, New York), we constructed a possible conformation for OOBPD and the molecular length in its most extended form was found to be 37.5 Å. This value is much larger than the apparent molecular length in the nematic phase. Thermal vibration of the long alkyl chains at the both ends of the rigid part may be a possible explanation of this shortening but formation of skewed cybotactic nematic groups can give a much better explanation. In the skewed cybotactic nematic phase molecules are ar-

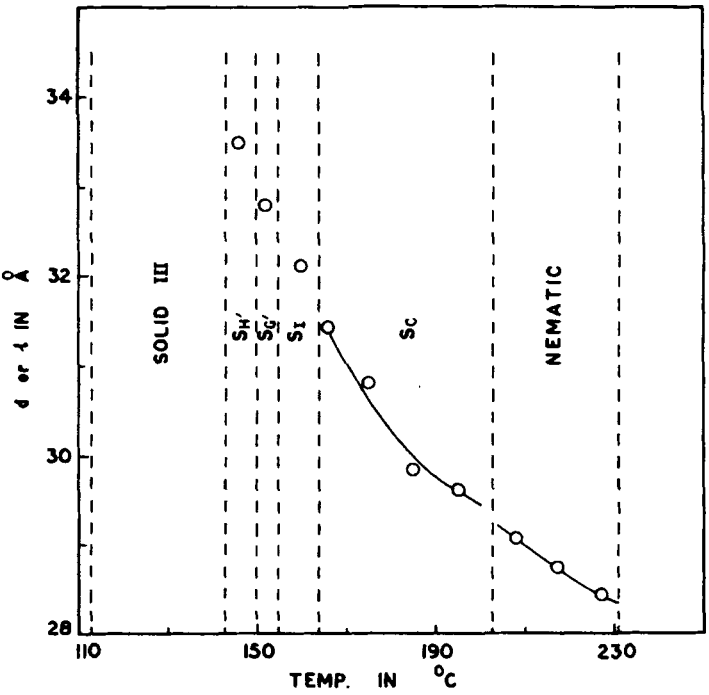

FIGURE 14 Variation of d and l with temperature for aligned sample.

ranged in groups in such way that the centres of the group lie in a well defined plane and normal to the plane makes an angle with the molecule.[14a,14b] l is thus the thickness of this cybotactic planes. In smectic phases also this difference may be due to the fact that the molecules are tilted with respect to the normals to the smectic layers. We define a tilt angle as

$$\beta_t = \cos^{-1}\left(\frac{x}{L}\right)$$

where L is the molecular length in its most extended conformation and $x = d$ for smectics and $x = l$ for cybotactic nematic. β_t increases with temperature as shown in Figure 15. This definition of β_t is of course somewhat arbitrary in that it includes any changes of internal conformation. It is often in good agreement with the angle measured directly from the diffraction patterns. In our case, only in S_C phase the angle β_t was directly measured from X-ray patterns. Since the angle between the outer and inner ring maxima in this phase (at

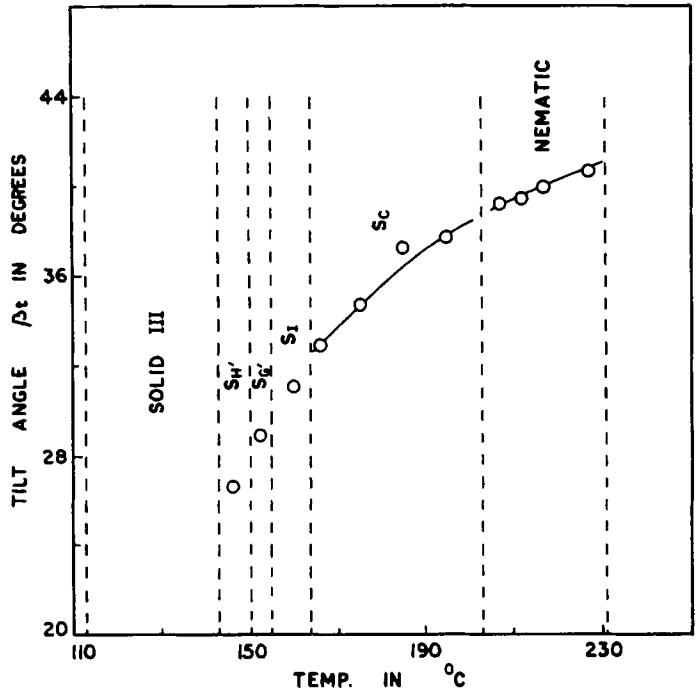

FIGURE 15 Variation of tilt angle β_t with temperature.

185°C) was found to be 77°, the deviation from non-orthogonality i.e. the tilt angle, according to our definition, would be 13° which is much lower than the value figured. Vibrations of the alkyl chain may be a reason for this discrepancy.

3.3 Order parameters and distribution function in the nematic phase

Variation of orientational order parameters $\langle P_2 \rangle$ and $\langle P_4 \rangle$ with temperature along with Maier-Saupe theoretical values are shown in Figure 16. Variations of normalised orientational distribution function $f(\beta)$ with the angle β at four different temperatures are given in Figure 17. Order parameters are calculated from the distribution function using the following relation

$$\langle P_L \rangle = \int_o^{\pi/2} P_L\,(\cos\beta) f(\beta) \sin\beta d\beta \Big/ \int_o^{\pi/2} f(\beta) \sin\beta d\beta$$

with $L = 2$ and 4. P_L (cos β) is the Legendre polynomial of L^{th}

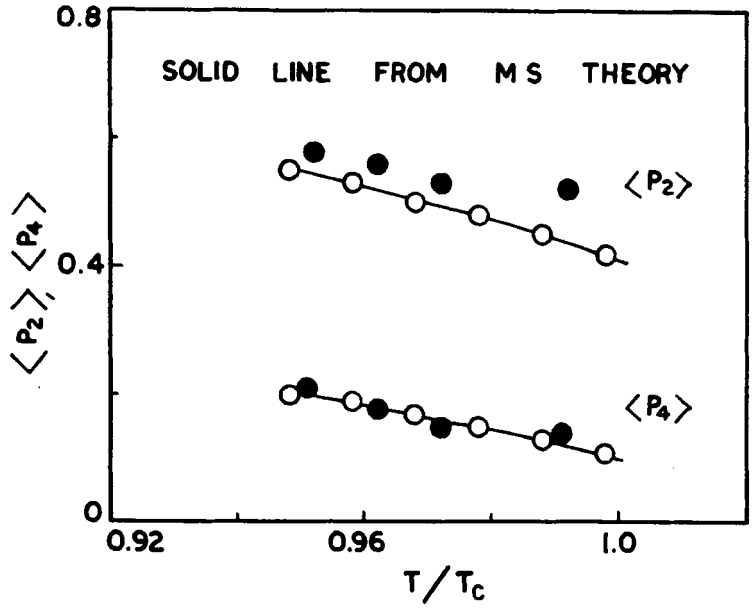

FIGURE 16 Orientational order parameters $\langle P_2 \rangle$ and $\langle P_4 \rangle$ against T/Tc.

degree. Again $f(\beta)$ is related to the intensity $I(\theta)$ along with the diffuse equatorial are by[17]

$$I(\theta) = \int_{\theta}^{\pi/2} f_d(\beta)\, \mathrm{see}^2\theta(\tan^2\beta - \tan^2\theta)^{-\frac{1}{2}} \sin\beta d\beta$$

$f_d(\beta)$ describes the distribution function for the orientation β of a small volume relative to the director $\hat{n}$ ($\beta = 0$) and is expected to be close to the singlet distribution function $f(\beta)$. A computer programme was written to calculate $f(\beta)$ using the experimental values of $I(\theta)$, the detail procedure has been described earlier.[18] Experimental $\langle P_2 \rangle$ and $\langle P_4 \rangle$ values are in good agreement with the theoretical values except at one temperature in the case of $\langle P_2 \rangle$.

The normalised singlet orientational distribution function is related to the pseudo-potential by the relation

$$f(\beta) = Z^{-1} \exp[-V(\beta)/kT] \tag{1}$$

Z being the partition function.

$f(\beta)$ is best fitted to the form

$$f(\beta) = \exp[\sum_{L\text{even}} a_L P_L(\cos\beta)] \tag{2}$$

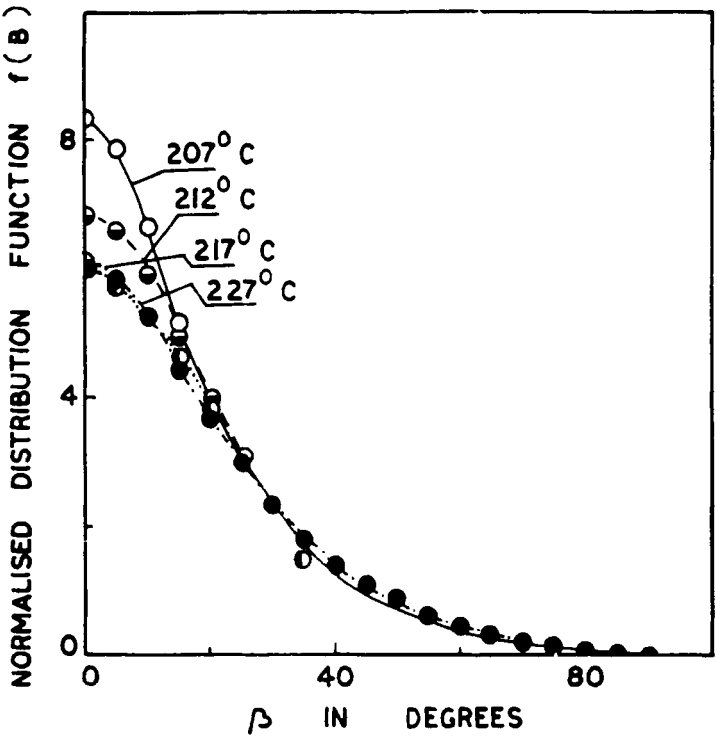

FIGURE 17 Normalised orientational distribution function $f(\beta)$ against angle β.

We have calculated the angular part of the mean field potential written in the form

$$V(\beta) = \sum_{L\,\text{even}} b_L \langle P_L \rangle P_L(\cos\beta)$$

b_L values are calculated from least squares fitting to $enf(\beta)$ values of equation (2). As in our previous papers,[18,19] the coefficients b_L are assumed to be temperature independent. Taking all the four temperature data, the pseudopotential can be written in the form (upto $L = 4$ term) (cf. HJL potential[20])

$$V(\beta)/kT = -(3241 \pm 261)\,\langle P_2 \rangle\, P_2\,(\cos\beta)$$

$$+(4553 \pm 1582)\,\langle P_4 \rangle\, P_4\,(\cos\beta)$$

Standard deviations of b_2 is reasonable while that of b_4 is large as in our previous findings.[18,19]

We could not calculate order parameters for the smectic C phase. The outer broadened maxima seemed to be due to the overlapping of two intensity maxima. We feel that the orientational ordering of the hydrocarbon chain is different from the ordering of the rigid portion of the molecule.[21] This calculation will be done later on.

Acknowledgment

We are thankful to U.G.C. for financial assistance and a Research Fellowship (P. Mandal).

References

1. Barrall II, E. M., Goodby, J. W. and Gray, G. W., *Mol. Cryst. Liq. Cryst.*, **49**, 319 (1979).
2. Goodby, J. W. and Gray, G. W., Proc. of a meeting held at Garmisch-Partenkirchen, 21–25 January, page 32, (1980).
3. Sparatt, W. and Schneider, G. M., *Mol. Cryst. Liq. Cryst.*, **51**, 101 (1979).
4. Demus, D. and Rurainski, R., *Mol. Cryst. Liq. Cryst.*, **16**, 171 (1972).
5. Arora, S. L., Taylor, T. R., Fergason, J. L. and Saupe, A., *J. Amer. Chem. Soc.*, **91**, 3671 (1969).
6. Jha, B. and Paul, R., *Proc. Nucl. Phys. & Solid State Phys. Symp.* (India), **19C**, 481 (1976).
7. H. P. Klug and L. E. Alexander, X-ray diffraction procedures for polycrystalline and amorphous materials, John Wiley and Sons, New York, Pages 114 and 473 (1974).
8. de Vries, A., Liquid Crystals, Pramana Supplement, No. 1, Edited by S. Chandrasekhar, Bangalore, 93 (1975).
9. Sackmann, H. and Demus, D., *Mol. Cryst. Liq. Cryst.*, **21**, 239 (1973).
10. Demus, D., Goodby, J. W., Gray, G. W. and Sackman, H., *Mol. Cryst. Liq. Cryst. Lett.*, **56**, 311 (1980).
11. S. Diele, D. Demus and H. Sackmann, *Mol. Cryst. Liq. Cryst. Lett.*, **56**, 217 (1980).

12a. de Vries, A., *Mol. Cryst. Liq. Cryst.*, **63**, 215 (1981).
12b. Gane, P. A. C., Leadbetter, A. J. and Wrighton, P. G., *Mol. Cryst. Liq. Cryst.*, **66**, 247 (1981).

13. Gane, P. A. C., Leadbetter, A. J., Wrighton, P. G., Goodby, J. W., Gray, G. W. and Tajbaksh, A. R., *Mol. Cryst. Liq. Cryst.*, **100**, 67 (1983).

14a. de Vries, A., *Mol. Cryst. Liq. Cryst.*, **10**, 31 (1970).
14b. de Vries, A., *Mol. Cryst. Liq. Cryst.*, **10**, 219 (1970).

15. de Vries, A., Ekachi, A. and Spielberg, N., J. Phys. Paris Colloque, **40C**, 147 (1979).
16. de Vries, A. and Quadri, S. B., Liquid Crystals, Proc. Int. Conf. Bangalore, Edited by S. Chandrasekhar, 179 (1979).
17. Leadbetter, A. J. and Norris, E. K., *Mol. Phys.*, **38**, 669 (1979).
18. Bhattacharjee, B., Paul, S. and Paul, R., *Mol. Phys.*, **44**, 139 (1981).
19. Bhattacharjee, B., Paul, S. and Paul, R., *Mol. Cryst. Liq. Cryst.*, **89**, 181 (1982).
20. Humphries, R. L., James, P. G. and Luckhurst, G. R., *J. Chem. Soc. Faraday Trans. II,*, **68**, 1031 (1972).
21. Paranjpe, A. S., *Mol. Cryst. Liq. Letters*, **82**, 93 (1982).